Efficient Local Reflectional Symmetries Detection

Tianqiang Yuan and Xiaoou Tang
Department of Information Engineering
The Chinese University of Hong Kong
Hong Kong
{tqyuan3, xtang}@ie.cuhk.edu.hk

***Abstract*—In this paper, we present a novel framework for efficient multiple reflectional symmetric regions detection in real images. First, we present a fast operator to measure the symmetry. Then based on the extracted edge image, the dilation and erosion operations are applied for potential regions. Finally, the symmetry axes are derived based on weighted Principle Component Analysis (PCA). The experiments based on the proposed algorithm show encouraging results on real images even with small size local symmetric regions and complex backgrounds.**

I. INTRODUCTION

Symmetry [5] is a salient and prolific appearance in man made or nature objects. It has attracted much attention in computer vision and pattern recognition. Symmetry detection has potential significance for general object detection, tracking, and recognition. In practice, it has been applied for face detection [11] and vehicle following [12]. Rotational symmetry [2][4][13] and reflectional symmetry are the two commonly studied symmetry types.

Reflectional symmetry is defined as an invariance of reflection to one straight line, denoted as reflection-symmetric axis. Many researches were concerned with reflectional symmetry detection. According to the features used for symmetry description, they can be classified into two main categories. One is based on edges and shapes of objects [6][8][9][15][16]. The main advantage of this category is that the edges and shapes are very efficient in computation; while the disadvantages of them include 1) the edges and shapes are not effective conditions for symmetry without successful segmentation; 2) when the background is complex and the objects are small, the symmetry of edges and shapes will be undistinguishable; and 3) stable edge detection is still an unsolved problem. The other category mainly uses the region–based techniques, *e.g.* complex comments [3], Fourier-Mellin representation [14], gradient orientation histogram [1], and global optimization with genetic algorithm [10]. The former two were used to detect global symmetries with rotations and they both have assumption that the center symmetries must be the center of images. To remove this constraint, Sun proposed a fast symmetry detection method with gradient orientation histogram [1]. It has the property of object location invariants but can only work in the cases with simple backgrounds. By using the genetic algorithm, Kiryati and Gofman proposed a global optimization approach to detect only one dominant local symmetric region in gray level images [10]. Smoothness constraints of its objective function and the initialization for small symmetry areas are still the bottlenecks.

By taking into account the position, symmetry scale, axis length, and orientation, reflectional symmetry detection faces the challenges in accuracy, robustness, and efficiency. Moreover, in many cases, the size of the local symmetric region is very small and background is complex, which make the problem more difficult. To tackle these issues, in this paper, we propose a general approach to detect multiple local reflectional symmetric regions in a gray level image. First, a region-based operator is proposed for efficient symmetry measurement of the points; then a serial of morphologic operations are conducted to select the potential regions and group the symmetry centers; finally we apply weighted Principle Component Analysis (PCA) algorithm [7] to detect the local symmetry axes. The algorithm is introduced in Section 2 and the experimental results are shown in Section 3. Finally, Section 4 concludes this paper.

II. EFFIEICENT LOCAL REFLECTIONAL SYMMETRIC REGIONS DETECTION

A. Symmetry measurement operator

In real images, objects are not absolutely symmetric to their axes with pixel reflectional computations due to the affections of illuminations, object distortion and images qualities. In this paper, the symmetry is measured as follows. For a center point (x, y), a circle with radius r is used to decide whether the region is symmetric, as shown in the Fig. 1(a). To reduce the computation, we use only the points on the circle to measure the symmetry. It is obvious that the smaller is the r, the more reasonable is the approximation. For better accuracy, we add some concentric circles as shown in Fig. 1(b).

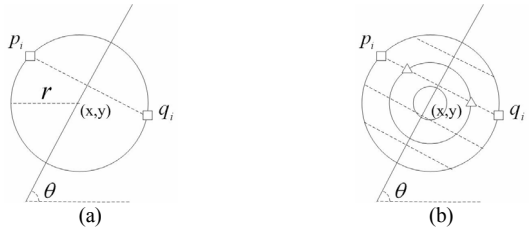

Fig. 1. Symmetry measurement. (a) with one circle; and (b) with multiple concentric circles.

0-7803-9134-9/05/$20.00 ©2005 IEEE

Assume a diameter with angle θ separates the circle into two point arrays $\{p_i\}$ and $\{q_i\}$, $i=1,2,\cdots,M$, where p_i and q_i are gray level values at the geometry symmetric point pair, and M is the number in each array. Then, the symmetry $Sc(x,y,\theta)$ is defined as:

$$Sc(x,y,\theta)=\sum_{i=1}^{M} Sp(p_i,q_i), \tag{1}$$

$$Sp(p_i,q_i)=\begin{cases}\dfrac{|p_i-q_i|}{\min(p_i,q_i)} & \dfrac{|p_i-q_i|}{\min(p_i,q_i)}\le Sp_{thre}\\ Sp_{thre} & \dfrac{|p_i-q_i|}{\min(p_i,q_i)}> Sp_{thre}\end{cases},$$

where Sp_{thre} is a truncation threshold.

B. Potential regions selection

As described above, the symmetry measurement does not have scale and rotation invariant properties. To alleviate the brute-force computation in every angle and scale, we first search for some potential regions.

Symmetry points are rich in images. Smooth areas satisfy the symmetry measurement, but mostly they are background or only parts of them have symmetry axes. Here we conduct the morphologic operations on edge image to obtain the potential regions. We use Sobel operator and apply it in separated blocks by using adaptive local thresholds to obtain the edge images, which makes the result more robust. Denote the derived edge image as E, we perform the dilation and erosion operations as:

$$E_d = E\oplus MS(r_d), \tag{2}$$

$$E_e = E_d\odot MS(r_e),$$

where $\oplus$ and $\odot$ are dilation and erosion operation respectively, $MS(*)$ is morphologic structure operator and its parameter is the operator size. Thus, r_d and r_e are the sizes of dilation and erosion operation respectively, and their range is set as $r<r_d<r_e<2r$ in our experiments. r_d is less than r_e so that

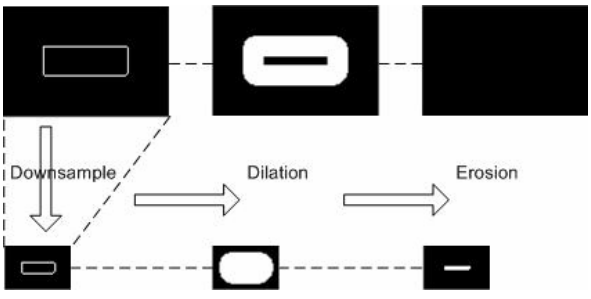

Fig. 2. Potential regions selection from multi-resolution morphologic operation.

The goal of dilation is to combine the close edges to potential regions and that of erosion is to remove the lonely edges and big scale shapes. Considering the computation of dilation and erosion, we use a small fixed operator only. For different scales, we reduce the size of image by some proportion, such as 1.2, and again perform the above morphologic operations with fixed r_d and r_e. As shown in Fig. 2, the left is edge images in each row. When the object is big, its edge or profile expands widely. After dilation, there are still leaks in its center as shown in the upper row of Fig. 2. r_e is greater than r_d so that we can remove all edges after the erosion. Thus, nothing is selected within the images of big resolution. In the downsampled images, there are no potential regions until the contour are suitable in the small size images. In Fig. 2, the right one in the bottom row contains the detected potential region.

C. Detection of symmetry axes

Denote the potential regions as PR, then

$$PR=\{(x,y)\,|\,E_e(x,y)=1\}, \tag{3}$$

We conduct the symmetry measurement operator in (1) within PR and on original image, where θ is preset.

How to detect local symmetry axis is the key problem for symmetry detection. Let

$$ES_T=\{(x,y)\,|\,(x,y)\in PR \quad \& \quad Sc(x,y,\theta)<T_{ES}\}, \tag{4}$$

$$PR_D = ES_T\,\tilde{\oplus}\,MS(r_L),$$

$$PR_T = PR_D\odot MS(r_L).$$

We set a symmetry threshold T_{ES} to select the candidate symmetry centers ES_T, and $\tilde{\oplus}$ in (4) means that a dilation operation with size r_L is performed on each ES_T so that the close points are grouped into a new region PR_D. By using the same method as in Section 2.A, we erode them to obtain shrunk potential regions PR_T, in which we detect a local symmetry axes. Fig 3 shows the details of the whole procedure.

(a) (b) (c) (d) (e)

Fig. 3. (a) A cropped image; (b) Potential region; (c) symmetry measurement; (d) Threshold truncation; (e) Shrunk local region.

Denote the point array in the shrunk local region as

$$\begin{cases}\{x_i,y_i,s_i\} \quad i=1,2,\cdots,N\\ where \quad (x_i,y_i)\in PR_T \quad \& \quad Sc(x_i,y_i,\theta)<T_{ES}\\ s_i=T_{ES}-Sc(x_i,y_i,\theta)\end{cases} \tag{5}$$

where N is the length of the array. In the following, we introduce how to apply Principle Component Analysis (PCA)

to detect the axes. Considering s_i as the weight for each point, we conduct weighted PCA as follows.

Mean points:

$$\begin{bmatrix} m_x \\ m_y \end{bmatrix} = \sum_{i=1}^{N} \left(s_i \cdot \begin{bmatrix} x_i \\ y_i \end{bmatrix} \right) \Big/ \sum_{i=1}^{N} s_i \ . \tag{6}$$

Covariance matrix:

$$C = \frac{1}{N} \sum_{i=1}^{N} s_i \begin{bmatrix} (x_i - m_x)(x_i - m_x) & (x_i - m_x)(y_i - m_y) \\ (x_i - m_x)(y_i - m_y) & (y_i - m_x)(y_i - m_y) \end{bmatrix}. \tag{7}$$

Eigenvalue decomposition:

$$C \begin{bmatrix} dx_i \\ dy_i \end{bmatrix} = \lambda_i \begin{bmatrix} dx_i \\ dy_i \end{bmatrix} \quad i = 1, 2 \ . \tag{8}$$

λ_i is the eigenvalue and $[dx_i, dy_i]^T$ is the corresponding eigenvector. The eigenvalue measures the information richness of orthogonal direction. Assume $\lambda_1 \geq \lambda_2$, then $[dx_1, dy_1]^T$ is the principle direction. In this paper, the conditions for symmetry existence include:

$$\begin{cases} \lambda_1 / (\lambda_1 + \lambda_2) > T_\lambda \\ \left| arctg(dy_1 / dx_1) - \theta \right| < T_\theta \end{cases}, \tag{9}$$

where T_λ is the threshold characterizing the energy ratio between two orthogonal directions, and T_θ is the difference limit between the angle of principle direction and the preset angle. When the conditions are satisfied, the symmetry axis is the line segment represented as

$$\begin{aligned} &[m_x, m_y]^T + \Delta [dx_1, dy_1]^T, \\ &\min_{(x_i, y_i)} (x_i dx_1 + y_i dy_1) \leq \Delta \leq \max_{(x_i, y_i)} (x_i dx_1 + y_i dy_1) \ . \end{aligned} \tag{10}$$

For more robustness with a high threshold, we use an iteration to test the above weighted PCA as following table.

Step 1: In (5), if N is too small, end the iteration.
Step 2: Process (6), (7) and (8)
Step 3: If (9) is satisfied, go to step 4; else, reduce T_{ES} and go to Step 1.
Step 4: Obtain a symmetry axis with (10).

III. EXPERIMENTS

A. Parameter setting and analysis

As described above, there are some parameters to be set for the whole algorithm. First, in Section 2.A, we use two concentric circles and set their radiuses as 5 and 3 respectively. And in (1), the truncation threshold Sp_{thre} is used to alleviate the effect of few asymmetry point pairs in symmetry areas. Oppositely, it also reduces the measurements of asymmetry areas. Fig. 4 shows the effect of variant Sp_{thre}, in which the example is the same as in Fig. 3. In the following experiments, we set $Sp_{thre} = 0.6$ experimentally for more distinguishing and continuous axes.

In Section 2.B, the morphologic structure operator $MS(r)$ is set as disk with radius r. As $r < r_d < r_e < 2r$, we set $r_d = 7$ and $r_e = 9$ to obtain less regions containing axes. With (4), we shrink the potential regions. T_{ES} is set as 0.15. The $MS(r_L)$ can be set as line with angle θ and $r_L = 2$. In the procedure of weighted PCA, $T_\lambda = 90\%$ and $T_\theta = 5^\circ$, which seems strict but are appropriate for the detections of regular objects, such as circle, square, and triangle. As shown in Fig. 5, green lines are symmetry axes of the objects. The reasons affect their accuracies are: 1) image size reducing and recovering; 2) the size of symmetry measurement is small, so that the interval of angles is big; 3) inaccuracy caused by PCA.

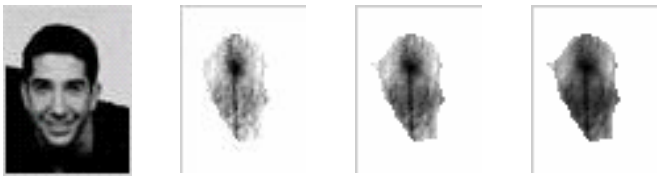

(a) (b) (c) (d)

Fig. 4. Effect of varying Sp_{thre} : (a) original image; (b) Sp_{thre} =0.3; (c) Sp_{thre} =0.6; and (d) Sp_{thre} =1.0.

(a) (b) (c)

Fig. 5. Detection of regular objects, $\theta = 90^\circ$.

B. Experimental Results

We illustrate two experimental results as shown in Fig. 6. In the experiments, θ is selected from 70° to 110° because mostly we care about vertical symmetry objects, such as faces. There is a salient face in Fig. 6(a). The background is complex and also contains symmetries. In Fig. 6(b), there are six small size faces with different rotation angles. We mark the symmetric regions with red rectangles and their center axes. It is encouraging that all faces can be detected by several scale symmetry measurement operators and their axes are very close. Besides, some symmetry regions are also detected in the following situations: 1) The regions contain symmetry objects; 2) The regions are parts of some objects and contain symmetry without close contour; 3) The regions are not symmetric due to failures of local region selections in complex background.

Searching in different scales and scales is robust but time-exhausting. Our experiments were conducted on a PC with 1.50GHz Pentium(R) IV CPU and 256M memory. As listed in Table 1, the speed is encouraging.

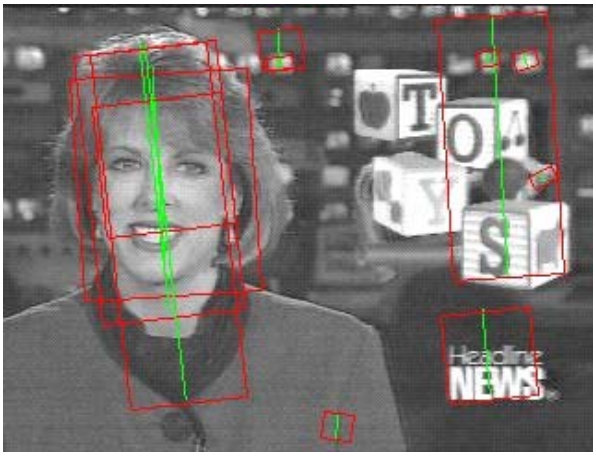

(a)

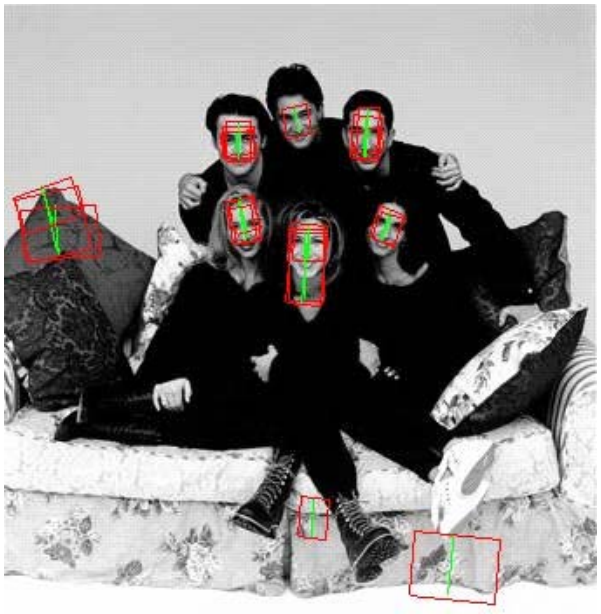

(b)

Fig. 6. Experimental results.

TABLE 1. EFFICIENCY OF EXPERIMENTS

Images	**Efficiency**		
	Image size	***Symmetry Number***	***Time (Second)***
Fig 6(a)	320×240	12	4.062
Fig 6(b)	340×350	21	4.235

IV. CONCLUSIONS AND FUTURE WORK

In this paper, we proposed a novel framework for multiple local reflectional symmetry regions detection in real images. The experimental results indicate that our proposed method can detect multiple local symmetric regions, even when their sizes are small. There are two major problems for our future work: 1) use more informative features for potential regions selection, such as close contour; and 2) improve the speed for real time detection and apply it to help face detection.

ACKNOWLEDGMENT

The work described in this paper was fully supported by grants from the Research Grants Council of the Hong Kong Special Administrative Region. The work was done while all the authors are with the Chinese University of Hong Kong.

REFERENCES

[1] C. Sun, "Symmetry Detection using Gradient Information," Pattern Recognition Letters, Vol. 16, No. 9, pp. 987-996, 1995.

[2] D. Reisfeld, H. Wolfson, and Y. Yeshurun, "Context Free Attentional Operators: the Generalized Symmetry Transform," IJCV, Vol. 14, pp. 119-130, 1995.

[3] D. Shen, H. Ip, K. Cheung, and E. Teoh, "Symmetry Detection by Generalized Complex (GC) Moments: A Close-Form Solution," IEEE Trans. PAMI, Vol. 21, No. 5, pp. 466-476, May 1999.

[4] G. Loy and A. Zelinsky, "Fast Radial Symmetry for Detection Points of Interest," IEEE Trans. PAMI, Vol. 25, No. 8, Aug. 2003.

[5] H. Weil, "Symmetry," Princeton University Press, 1952.

[6] H. Zabrodsky, S. Peleg, and D. Avnir, "A Measure of Symmetry Based on Shape Similarity," IEEE CVPR, pp. 703-706, 1992.

[7] K. Fukunaga, "Statistical Pattern Recognition," Academic Press, 1990.

[8] M. Kelly, and M. Levine, "Annular Symmetry Operators: Locating and Describing Objects," IEEE ICCV, pp. 1016-1021, June 1995.

[9] M. Su and C. Chou, "A Modified Version of the K-Means Algorithm with a Distance Based on Cluster Symmetry," IEEE Trans. PAMI, Vol. 23, No. 6, June 2001.

[10] N. Kiryati and Y. Gofman, "Detecting Symmetry in Gray Level Images: The Global Optimization Approach," IJCV, Vol. 29, pp. 29-45, 1998.

[11] Sun, W. Huang, and J. Wu, "Face Detection Based on Color and Local Symmetry Information," IEEE AFGR, pp. 130-135, April 1998.

[12] Y. Du and N. Papanikolopoulos, "Real-time vehicle following through a novel symmetry-based approach," IEEE International Conference on Robotics and Automation, Vol. 4, pp. 3160-3165, April 1997.

[13] G. Heidemann, "Focus-of-attention from local color symmetries," IEEE Trans.PAMI, Vol. 26, No. 7, pp. 817-830, July 2004.

[14] Derrode and F. Ghorbel, "Shape analysis and symmetry detection in gray-level objects using the analytical Fourier-Mellin representation," Signal Processing, Vol. 84, No. 3, pp. 25-39, 2004.

[15] V. Prasad and B. Yegnanarayana, "Finding Axes of Symmetry from Potential Fields," IEEE Transa. Image Processing, Vol. 13, No. 12, pp. 1559-1566, Dec. 2004.

[16] H. Wang and D. Suter, "LTSD: A Highly Efficient Symmetry-Based Robust Estimator," International Conference on Control, Automation, Robotics and Vision, Vol. 1, pp. 332-337, 2002.